

Aus dem Zentrum für Zahn-, Mund- & Kieferheilkunde
der Medizinischen Fakultät Charité – Universitätsmedizin Berlin

DISSERTATION

Evaluation of the plaque affinity of different PEEK grades in comparison to titanium and zirconium dioxide

zur Erlangung des akademischen Grades

Doctor medicinae dentariae (Dr. med. dent.)

vorgelegt der Medizinischen Fakultät
Charité – Universitätsmedizin Berlin

von

Modar Othman

Datum der Promotion: 25.06.2023

Contents

List of abbreviations	3
List of figures	4
List of tables	5
Abstract	6
Abstract	7
1.Introduction	8
1.1 <i>Oral Biofilm and Peri-implantitis</i>	<i>10</i>
1.2 <i>Dental Implant materials.....</i>	<i>14</i>
1.2.1 <i>Titanium-based dental implants</i>	<i>14</i>
1.2.2 <i>Ceramics as Dental Implant materials</i>	<i>17</i>
1.2.3 <i>PEEK as potential material for dental implants</i>	<i>19</i>
2. Materials and Methods.....	20
2.1 <i>Sample preparation.....</i>	<i>20</i>
2.2 <i>Surface characterization.....</i>	<i>23</i>
2.2.1 <i>Surface Roughness.....</i>	<i>23</i>
2.2.2 <i>Contact Angle</i>	<i>23</i>
2.3 <i>Microbiological culture</i>	<i>24</i>
2.4 <i>Fluorescence microscopy of bacterial colonies</i>	<i>28</i>
Principles of fluorescence microscopy.....	28
2.5. <i>Statistical analysis:</i>	<i>33</i>
3. RESULTS.....	34
3.1 <i>Surface characterization.....</i>	<i>34</i>
3.1.1 <i>Surface Roughness measurements.....</i>	<i>34</i>
3.1.2 <i>Contact Angle measurements.....</i>	<i>36</i>
3.2. <i>Biofilm Formation</i>	<i>38</i>
4. Discussion.....	41
5. Conclusion	44
6. References	45

List of abbreviations

PEEK	Polyetheretherketone
Gpa	Gigapascals
Y-TZP	Yttrium stabilized tetragonal zirconia polycrystals
Mpa	Megapascal
CAD/CAM	Computer-aided Design & Computer-aided Manufacturing
S sanguinis	Streptococcus Sanguinis
P-PEEK	Pure implantable PEEK material (i4-R)
R-PEEK	Red dental PEEK grade (DC4470 R)
W-PEEK	White dental PEEK grade (DC4420)
B-PEEK	Beige dental PEEK grade (DC4450)
Ti	Implantable titanium grade
Zr	Implantable zirconium dioxide grade
SiC	Silica carbide papers
R _a	The mean roughness
DSM	German collection of Microorganisms and cell cultures
TSB	Trypticase Soy Broth
(OD ₆₀₀)	The optical density at wavelength 600 nm
(PBS)	Phosphate buffered saline
FDA	Fluorescein diacetate
Nm	Nanometer
Sd	Standard deviation

List of figures

FIGURE 1: THE BIOFILM FORMATION STEPS.	10
FIGURE 2: THE ACQUIRED PELLICLE AND THE BACTERIAL ADHESION.	11
FIGURE 3: DEVELOPMENT OF PERI-IMPLANTITIS AND THE IMPLANT FAILURE.	13
FIGURE 4: THE IMPLANT SHOULDER SHIMMERS GRAYISH THROUGH THE THIN MUCOSA.	16
FIGURE 5: DIFFERENT TYPES OF CERAMIC IMPLANTS FROM STRAUMANN.	17
FIGURE 6: THE CERAMIC FURNACE (THERMO STAR, THERMO-STAR GMBH, AACHEN, GERMANY) USED FOR SINTERING THE Zr SAMPLES.	21
FIGURE 7: THE POLISHING MACHINE (EXAKT 400 CS, EXAKT ADVANCED TECHNOLOGIES GMBH, NORDERSTEDT, GERMANY) USED TO POLISH THE SAMPLE SURFACES.	22
FIGURE 8: PROCEDURE OF THE SURFACE ROUGHNESS MEASUREMENT USING THE ALICONA INFINITE FOCUS SYSTEM (ALICONA IMAGING GMBH, RAABA/GRAZ, AUSTRIA).	23
FIGURE 9: EXEMPLARY CONTACT ANGLE MEASUREMENT.	24
FIGURE 10: THE PHOTOMETER (BIOPHOTOMETER PLUS, EPPENDORF AG, HAMBURG, GERMANY) WHICH WAS USED TO OBTAIN A BACTERIAL CONCENTRATION IN THE TSB MEDIUM.	26
FIGURE 11: THE CELL STAINING MECHANISM USING FDA.	28
FIGURE 12: FLUORESCENCE MICROSCOPIC IMAGE OF <i>S. SANGUINIS</i> COLONIES AFTER INCUBATION WITH FDA FOR 30 MINUTES.	29
FIGURE 13: THE FLUORESCENCE MICROSCOPE (VANOX TAH-2 DIC, OLYMPUS EUROPA SE & CO. KG, HAMBURG, GERMANY), WHICH WAS USED TO VISUALIZE THE <i>S. SANGUINIS</i> COLONIES AFTER 18 HOURS OF INCUBATION.	30
FIGURE 14: FLUORESCENCE MICROSCOPIC IMAGES OF <i>S. SANGUINIS</i> COLONIES ON W-PEEK INCUBATED WITH FDA FOR 30 MINUTES, BEFORE EDITING (LEFT) AND AFTER EDITING (RIGHT).	31
FIGURE 15: DUE TO THE IMAGE PROCESSING IN IMAGEJ, THE COLONIES ON THE FLUORESCENCE IMAGES (HERE ON W-PEEK) SHOW AS RED AREAS, WHICH ARE COUNTED BY THE SOFTWARE.	32
FIGURE 16: BOXPLOT OF THE SURFACE ROUGHNESS OF THE DIFFERENT GROUPS.	35
FIGURE 17: EXEMPLARY WATER CONTACT ANGLES OF THE DIFFERENT GROUPS.	36
FIGURE 18: BOXPLOT OF THE WATER CONTACT ANGLES OF THE DIFFERENT GROUPS.	37
FIGURE 19: EXEMPLARY FLUORESCENCE MICROSCOPIC IMAGES OF THE DIFFERENT GROUPS AFTER 18 HOURS OF INCUBATION OF <i>S. SANGUINIS</i> COLONIES, BEFORE (LEFT) AND AFTER EDITING (RIGHT).	38
FIGURE 20: BOXPLOT OF THE NUMBER OF ADHERENT COLONIES OF THE DIFFERENT GROUPS. (**) SIGNIFICANTLY DIFFERENT TO W-, B- AND P-PEEK.	40

List of tables

<i>TABLE 1: COMPARISON OF THE CHEMICAL COMPOSITIONS BETWEEN TITANIUM GRADES (1-4).....</i>	<i>15</i>
<i>TABLE 2: SUMMARY OF THE SURFACE ROUGHNESS (Ra) OF THE DIFFERENT GROUPS (MEAN ± SD).</i>	<i>34</i>
<i>TABLE 3: SUMMARY OF THE WATER CONTACT ANGLE MEASUREMENTS OF THE DIFFERENT GROUPS (MEAN ± SD).</i>	<i>37</i>
<i>TABLE 4: SUMMARY OF THE ADHERENT COLONIES ON THE SURFACES OF THE DIFFERENT GROUPS.</i>	<i>39</i>

Abstract**Objective:**

The aim of this *in vitro* study was to investigate the formation of biofilms on the surfaces of materials applied for the fabrication of implant abutments and dental materials.

Materials and methods:

Specimens were prepared from six different materials: three types of dental grade Polyetheretherketone (PEEK), one type of implant-grade PEEK, one type of titanium implant abutment material, and one type of zirconium dioxide implant abutment. All specimens were subjected to initial surface polishing using grit rotating silicon carbide papers. Surface roughness measurements were conducted with an Alicona infinite focus system, and contact angle measurement were conducted on a Keyence V5000 digital microscope. Bacterial species *Streptococcus sanguinis* was cultured on the surfaces of the different materials for 18 hours and subsequently quantified by fluorescence microscope after fluorochrome staining with fluorescein diacetate.

Results:

Surface roughness measurement showed that titanium had the lowest surface roughness and the contact angle measurement showed that zirconium dioxide had the lowest mean contact angle. Biofilm formation was stronger on the surfaces of titanium and zirconium dioxide compared to the different PEEK materials.

Conclusion:

Within the limitations of a laboratory study, the quantification of biofilm formation on different types of materials showed that implant-grade PEEK material led to significantly lower amounts of adherent *S. sanguinis* colonies on its surface, and could therefore, in regard to biofilm formation, perform as well as titanium and zirconium dioxide when used as an implant dental material. However, clinical studies are necessary to corroborate these results.

Abstract

Zielsetzung:

Ziel dieser In-vitro-Studie war es, die Bildung von Biofilmen auf den Oberflächen von Materialien zu untersuchen, die zur Herstellung von Implantatabutments und Dentalmaterialien verwendet werden.

Materialien und Methoden:

Die Proben wurden aus sechs verschiedenen Materialien hergestellt, drei Arten von Polyetheretherketon zu der dentalen Verwendung (PEEK), eine Art von PEEK Implantieren, eine Art von Implantat-Abutment-Material Titan und eine Art von Implantat-Abutment-Zirkoniumdioxid. Alle Proben wurden poliert unter Verwendung von rotierenden Siliciumcarbidpapieren mit Körnung unterzogen. Oberflächenrauheitsmessungen wurden mit einem Alicona-Endlosfokussystem durchgeführt, Kontaktwinkelmessungen wurden mit einem digitalen Keyence V5000- Mikroskop durchgeführt. Die Bakterienspezies *Streptococcus Sanguinis* wurde 18 Stunden lang auf den Oberflächen der verschiedenen Materialien kultiviert und anschließend nach Fluorochrom-Färbung mit Fluoresceindiacetat durch ein Fluoreszenzmikroskop quantifiziert.

Ergebnisse:

Die Messung der Oberflächenrauheit zeigte, dass Titan die niedrigste Oberflächenrauheit aufwies, und die Messung des Kontaktwinkels zeigte, dass Zirkoniumdioxid den niedrigsten mittleren Kontaktwinkel aufwies. Die Biofilmbildung war auf den Oberflächen von Titan und Zirkoniumdioxid im Vergleich zu den verschiedenen PEEK-Materialien stärker.

Konklusion:

Im Rahmen einer Laborstudie zeigte die Quantifizierung der Biofilmbildung auf verschiedenen Materialtypen, dass PEEK-Implantat-Material zu signifikant geringeren Mengen anhaftender *S. Sanguinis*-Kolonien auf seiner Oberfläche führte und daher im Hinblick auf die Biofilmbildung eine Leistung erbringen konnte sowie Titan und Zirkoniumdioxid bei Verwendung als Implantat-Dentalmaterial. Es sind jedoch klinische Studien erforderlich, um diese Ergebnisse zu bestätigen.

1.Introduction

The human oral cavity is the gateway of the body and is in constant contact with the external environment because it is the first organ of the digestive system which all foods and beverages come through (45). Since the very first moment of birth, it is a favorable place for microbial colonization, where ideal temperatures and rich nutrient supply are the basis of the fast development of a large number of different bacterial species resulting in different types of biofilms, which in the presence of teeth and their surrounding gingival pockets are referred to as dental plaque (2).

Dental plaque, as defined by its microbial composition, can, for example, lead to periodontal diseases such as gingivitis as the simplest form, which, when untreated, results in periodontitis as a result of the interactions and the infection process between the commensal bacteria species which give our microflora a positive feature, and the pathogenic species which are recognized as the key etiologic factor for oral diseases (3).

Periodontitis is defined as a complex chronic inflammatory infectious disease, related to specific bacterial species such as *Aggregatibacter actinomycetemcomitans* and *Porphyromonas gingivalis*, and it can be increased by the presence of risk factors such diabetes and smoking, affecting the gingival tissues and potentially leading to tooth loss (4).

In the process of plaque formation, the adhesion of the early colonizing bacteria (for example, *Streptococci* such as *S. mutans*, *S. gordonii* and *S. mitis*) to the tooth surfaces is considered the crucial step for biofilm formation, followed by the adhesion of later colonizers forming a more mature oral biofilm (5).

Peri-implantitis, the inflammation equivalent of periodontitis on implants, is defined as a chronic inflammation that affects the implant-supporting soft and hard tissues (6). "Mucositis" represents the initial inflammation of this pathogenesis, which is reversible and does not cause bone loss, while "peri-implantitis" represents the advanced form of inflammation, which is usually established over a longer period of time with crestal peri-implant bone loss (7).

Dental implants have lately been used as a reliable solution to replace the missing teeth, and they act as an artificial tooth root that later helps the regaining of the function and the shape of the missing teeth (8), supporting the different types of fixed (9) and removable dentures (10).

Titanium and its alloys have been for a long time the material of choice for dental implants (11), however the high elasticity module and the esthetic needs led to the search for alternatives, and the most used alternatives were ceramics such as zirconia and lately polymers such as PEEK (polyetheretherketone) (12).

Polyetheretherketone (PEEK) is a high-performance polymer that was introduced to the market in the 1980s and was approved as implant material by the American Food and Drug Administration (FDA) in the 1990s (13).

Its outstanding material properties, such as high biocompatibility, chemical resistance and mechanical behavior, make it an interesting biomaterial for medical (14) and dental applications (15). Due to its high mechanical properties, which can be adjusted, e.g., by reinforcement with carbon fibers, PEEK has been proposed as a substitute for metallic biomaterials (16). Therefore, PEEK could also serve as a viable alternative to titanium and zirconia in the field of dental implantology.

1.1 Oral Biofilm and Peri-implantitis

Biofilm is defined as a complex, relatively undefinable microbial community developed on the tooth surface or any hard non-shedding surfaces immersed in an aqueous environment (17). In the mouth, the biofilm formation on the tooth surface is called dental plaque, whereas this microbial community can be formed and attached on other surfaces such as prosthetic restorations and dental implants. This formation is considered a major step in the development of the pathological process (18) of the most prevalent oral infections, such as periodontitis and dental caries, which are two of the most common infections in the oral cavity (19).

Biofilm formation starts with three major steps: attachment, colonization and biofilm development (20; Figure 1).

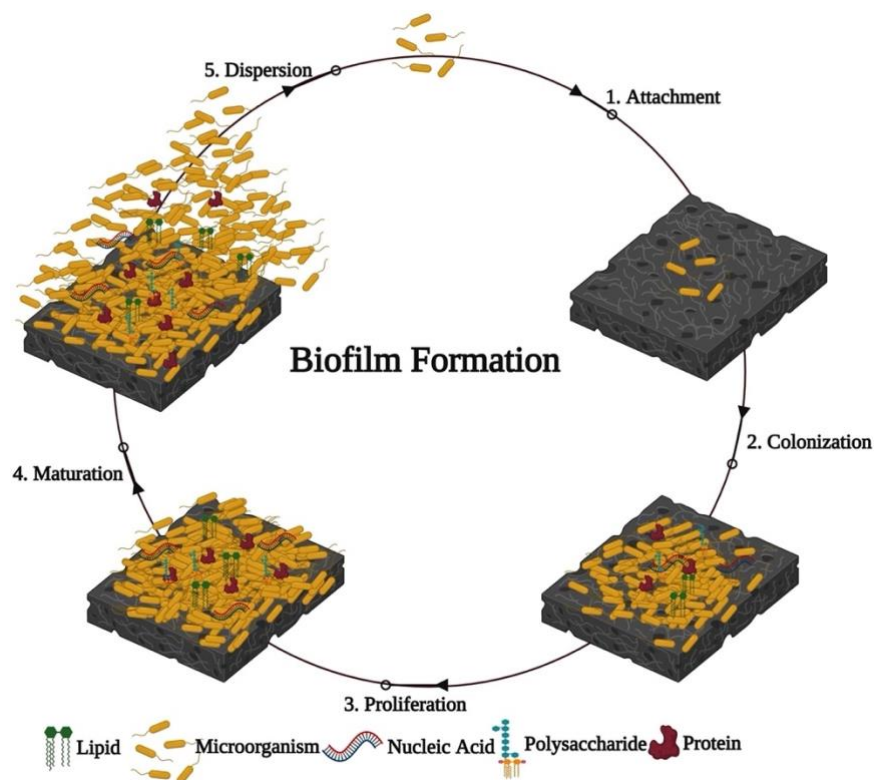


Figure 1: The Biofilm Formation Steps.

(The image was taken from the website https://www.frontiersin.org/files/Articles/676458/finicb-12-676458-HTML/image_m/finicb-12-676458-g001.jpg).

Seconds after tooth brushing, the surfaces of teeth, dental implants and gingivae/mucosa are covered by saliva, serum and other components secreted into the oral cavity by the salivary glands such as proteins (21). These components, and especially those coming from the saliva, represent a major nutrient source for the oral bacteria and additionally help the bacteria to attach to the aforementioned surfaces, due to the adsorption of the different salivary proteins (proline-rich proteins, mucin, IgA, etc.), which form a thin layer called the acquired pellicle (22).

The acquired pellicle plays a crucial role in conditioning the surface by altering the charge and free energy of the surface, leading to an increase in the efficiency of the bacterial adhesion, acting like an adhesion layer between the surface and the bacteria (23).

The initial colonizers colonize the entire tooth surface within 4 hours after pellicle formation. This binding between the bacterial surface and the surface of the pellicle is made possible by special surface molecules (adhesin) present on the surface of the bacterial cell (24; Figure 2).

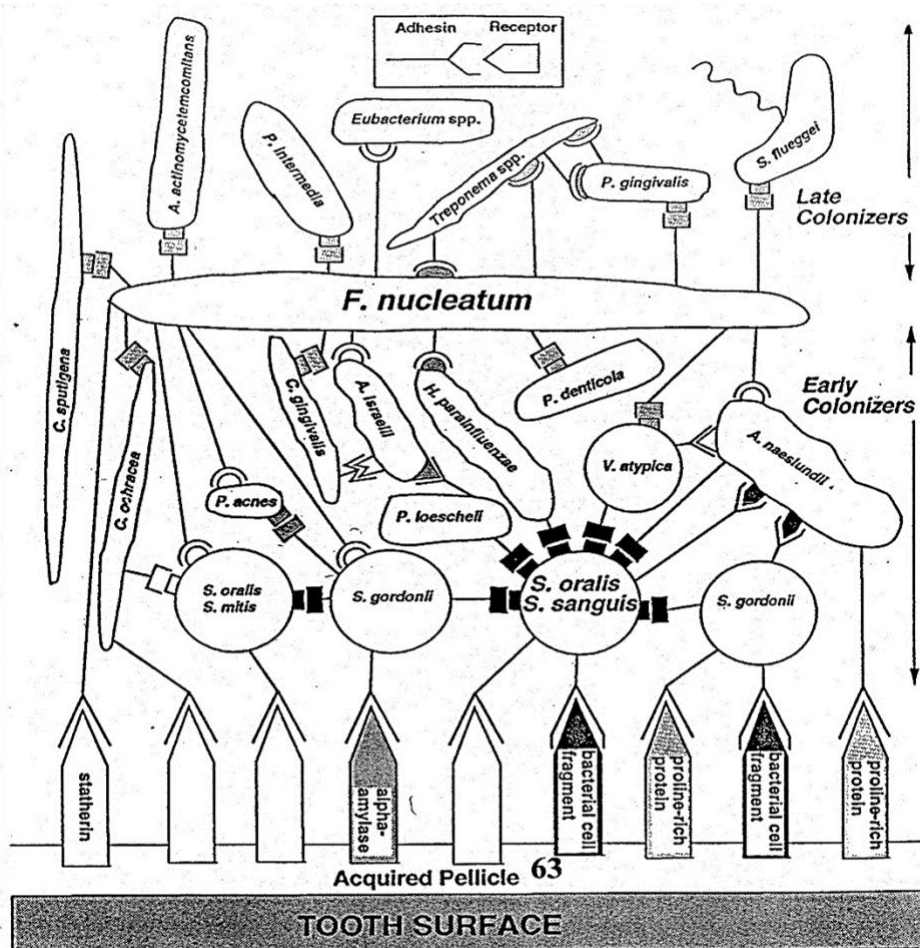


Figure 2: The Acquired Pellicle and The Bacterial Adhesion.

(The image was taken from the website <http://mikrolife.blogspot.com/2007/11/plaque-biofilm-formation.html?m=0>).

After the process of the initial colonization, the initial colonizers, represented by *streptococci* (*Streptococcus sanguinis*, *Streptococcus oralis*, *Streptococcus mitis*, etc.), help the other bacterial species that are unable to attach directly to the tooth surface to attach to the initial colonizers via a cell-cell interaction using the receptors on the surfaces of the initial colonizers, ultimately creating the dental biofilm (25).

About 30 minutes after the installation of a dental implant in the oral cavity, it will be covered with a pellicle layer (26) and the subsequent microbial colonization of the implant surface is analogous to the biofilm formation on tooth surfaces (27) - in brief, the bacteria colonize the surfaces of the implant and produce an extracellular polymeric matrix, which is responsible for creating microenvironments and changing the virulence of the bacteria (28). Under healthy conditions, the biofilm on implant surfaces is mainly composed of gram-positive aerobic bacteria (*Streptococci*) and a low number of periodontopathogenic bacteria (29,30). The periodontal pathogens are very similar to the microbiota species which are found in cases of periodontitis (*P. gingivalis*, *P. intermedia*, etc.) and are also mainly responsible for peri-implantitis (31).

Peri-implantitis is a pathogenic condition representing one of the main reasons for implant loss (32). Peri-implantitis is usually observed 5-11 years after implant insertion affecting both soft and hard tissues surrounding the implant (33).

This pathological process starts with the inflammation of the soft tissues around the implant associated with characteristic clinical symptoms such as bleeding on probing (BOP), and changes of the color (from pink to dark red) and the contour of the mucosal margin due to swelling. This condition is defined as peri-implant mucositis and occurs in 43 % of patients according to recent studies (34). This inflammation is not associated with bone loss and reversible under treatment, and it can be gone with time under healthy conditions (35). Without treatment, mucositis triggered by the resumption of the unhealthy conditions surrounding the implant tissues can cause loss of connective tissues, followed by the breakdown of the mucosal seal, permitting pathogenic bacteria to invade and start a new inflammatory process, which finally causes marginal bone loss around the implant and thus the formation of peri-implant pockets (36). This pattern is called peri-implantitis and its prevalence is increasing considerably, with 20 % of implants developing peri-implantitis (37; Figure 3).

Peri-implantitis is a multifactorial disease - for example, periodontitis in a patient's history, smoking and diabetes are general risk factors for peri-implantitis (38). However, it is believed that the early colonizers play a specific role for the establishment of peri-implantitis, whereas recent studies of subgingival and submucosal plaque samples in peri-implantitis showed the great presence of streptococcal species, including *streptococcus sanguinis* (39).

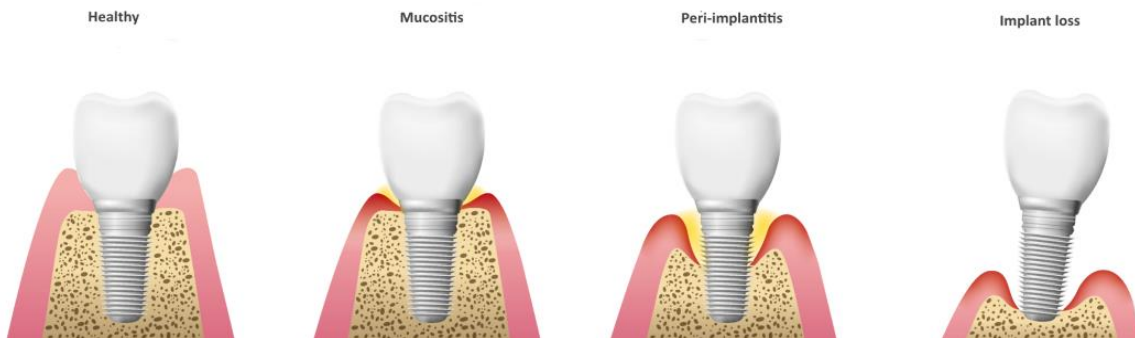


Figure 3: Development of Peri-implantitis and the implant failure.
(The picture was taken from <https://www.micro-ident.de/en/dentists/peri-implantitis/>).

1.2 Dental Implant materials

Replacing missing teeth has always been of major interest in the dental field, so that oral implants have undergone several changes throughout the decades. The Mayan civilization and the Egyptians were the first in history to replace missing teeth using different materials, for example, mussels, bone, wood and even other extracted teeth (40).

Ever since, implant manufacturing has followed the clinical need to obtain implants of biocompatible materials with good physical and chemical properties to enhance long-term success due to resistance against corrosion, fracture and wear (41). Nowadays, dental implants can be categorized according to their design, shape, function and the implant material, though implants are conventionally made of titanium (Ti) and titanium alloys (42-46).

1.2.1 Titanium-based dental implants

For more than five decades, titanium dental implants have been the most widely used metal-based implants. This began in the 1960s, after Swedish scientist Professor Brånemark discovered the potential of titanium implants to cause bone growth towards the implant surface and thus a strong connection with the surrounding bone. He defined this phenomenon as “osseointegration” (47). Titanium materials are available in two different forms. On the one hand as pure metal, the so-called commercially pure titanium (CpTi). On the other hand as titanium alloys to improve the material's properties (48). According to the American Society of Testing Materials (ASTM), pure titanium can be divided into 4 grades (Grade I-IV) depending on the amount of trace elements within pure titanium, such as carbon, iron, oxygen and nitrogen (49; Table 1).

Table 1: Comparison of the chemical compositions between Titanium grades (1-4).

(The table was taken from https://www.zapp.com/fileadmin/_documents/Downloads/materials/high_performance_alloys/de/Titan-Grade-1-4-Datenblatt.pdf)

	Fe	C	N	O	H	Ti
Ti 1	0.20	0.08	0.03	0.18	0.015	Rest
Ti 2	0.30	0.08	0.03	0.25	0.015	Rest
Ti 3	0.30	0.08	0.05	0.35	0.015	Rest
Ti 4	0.50	0.08	0.05	0.40	0.015	Rest

The reason that titanium and its alloys have long been the materials of choice is because of their excellent physicochemical properties, high biocompatibility, corrosion resistance and high strength (50). However, titanium has a high Young's modulus of 110 GPa, which is higher than that of enamel (80 Gpa), cortical bone (14 Gpa) and dentin (20 Gpa) (51). This mismatch between titanium and the surrounding bone during load transfer is thought to cause stresses at the implant-bone interface, leading to bone damage and consequent bone loss due to overload (52).

In addition, there have been some concerns that titanium may cause hypersensitivity reactions. On the one hand, this hypersensitivity could be explained as a result of an excessive pro-inflammatory reactivity of the tissue macrophages (53), or as a result of the release of metal ions from the implant following contact with skin or with the mucosa, whereby these ions react with some proteins turning them into allergens (54). On the other hand, due to the grey color of titanium, when placed in the esthetic zone in the presence of a thin gingival biotype, the grey appearance of titanium may be visible through the peri-implant tissues, thus impairing the esthetic outcome (55; Figure 4).



*Figure 4: The implant shoulder shimmers grayish through the thin mucosa.
(The picture was taken from <http://centralparkperio.com/naturalpinkdentalimplants.php>)*

1.2.2 Ceramics as Dental Implant materials

As a metal-free substitute for titanium, ceramics are being used in the field of implant dentistry, whereas implants made of aluminum oxide (“Tübingen implants”) are considered as the first generation of ceramic implants, which were withdrawn from the market in the early 1990s because of many factors such as their low fracture toughness and what they exhibit regarding linear elastic behavior (56). After aluminum oxide, Zirconia (Zirconium dioxide) was used due to its superior biomechanical properties, wear resistance and high flexural strength (80-100 Mpa) (57; Figure 5).



Figure 5: Different Types of Ceramic Implants from Straumann.

(The picture was taken from https://straumannprod-h.assetsadobe2.com/is/image/content/dam/sites/straumann/xy/dental-professionals/cgi/key-visuals-product-detail-pages/K0013-01_V01-SNOW-PURE%20Implant%20System_RGB_Transparent.png?fmt=png-alpha&wid=720).

Zirconium dioxide was first used for the fabrication of crowns and implant abutments (58,59). Yttrium-stabilized tetragonal zirconia polycrystals (Y-TZP), in comparison to other ceramics, have better mechanical properties related to the tetragonal-to-monoclinic phase transformation (60)

It has also attracted considerable attention and has been proposed as a viable dental implant material due to the white and opaque color of zircon, along with early reports of good biocompatibility and low affinity to bacterial plaque, which made it a material of interest in biomedical sciences (61).

On the one hand, zirconium dioxide showed preferable properties over titanium, such as favorable color and lower plaque affinity (62,63), combined with comparable osseointegration behavior to titanium-based implants (64,65). On the other hand, zirconium dioxide has a Young's modulus of around 210 GPa (66), which is higher than that of titanium, and thus even more detrimental than titanium implants in terms of overloading of the peri-implant bone.

1.2.3 PEEK as potential material for dental implants

Another group of materials in dentistry are polymers, which has recently included the high-performance polymer PEEK for the manufacture of dental prostheses.

PEEK is a semi-crystalline linear polycyclic thermoplastic (67). It has a high melting temperature of 343°C, allowing steam sterilization as well as gamma-radiation (68). It has been used in orthopedics and trauma as an alternative to metal-based implant materials (69) and exhibits less stress shielding (the stress removal which occurs due to the differences of the properties between the bone and the implant) (70) compared to stiff implant materials, due to its Young's modulus being closer to that of cortical bone (3-4 GPa), which can be adjusted, e.g., with reinforcing carbon fibers to around 18 GPa or with glass fibers to around 12 GPa (71,72). The combination of its metal-free property and its adjustable elastic modulus has led to the assumption that PEEK could represent a viable alternative implant material. It has so far been used as abutment material for provisional implant restorations (73), and also for definitive prosthetic restorations manufactured via CAD/CAM and pressing techniques (74). In comparison to titanium, PEEK has showed less hypersensitivity and less allergic reactions (75). Also, the grey/beige color of pure PEEK is closer to tooth colors and can be adjusted by adding pigment powders, making it more suitable for applications in esthetic regions (76), and additionally to that, some studies showed that PEEK has the ability to reduce the bacterial growth on its surface as it has been used in orthopedics without the need to use antibiotics (77). In addition to the mechanical factors influencing the implant complex, bacterial adhesion as a favoring factor for the development of peri-implantitis affects the long-term success of implants.

Therefore, the aim of the present study was to evaluate the colonization behavior of *S. sanguinis* as early colonizer on different PEEK grades compared to titanium and zirconia.

2. Materials and Methods

2.1 Sample preparation.

Six different materials were used, each forming a group:

- a pure implantable PEEK grade (“P-PEEK”), supplied as a round rod with 3 m length and a diameter of 10 mm (i4 R, Evonik industries, Essen, Germany)
- a red dental PEEK grade (“R-PEEK”), supplied as a blank with 98.4 mm diameter and 12 mm thickness (DC4470 R, Evonik industries, Essen, Germany)
- a white dental PEEK grade (“W-PEEK”), supplied as a blank with 98.4 mm diameter and 12 mm thickness (DC4420 R, Evonik industries, Essen, Germany)
- a beige dental PEEK grade (“B-PEEK”), supplied as a blank with 98.4 mm diameter and 12 mm thickness (DC4450 R, Evonik industries, Essen, Germany)
- an implantable titanium grade (“Ti”), supplied as round rod with 0.2 m length and a diameter of 10 mm (Friatec AG, Mannheim, Germany)
- an implantable zirconium dioxide grade (“Zr”), supplied as a blank with a 98 mm diameter and 18 mm thickness (MicroCeram GmbH, Meißen, Germany).

For each material, $n=10$ specimens were manufactured. For P-PEEK, round disc-shaped specimens with a diameter of 10 mm were obtained by cutting slices with a thickness of 2 mm from the round rod using a diamond saw (IsoMet 1000 Precision Cutter, Buehler, Lake Bluff, USA). For R-, W- and B-PEEK, square samples with an edge length of 10 mm and a thickness of 2 mm were manufactured from the blanks using the diamond saw. For Ti, round disc-shaped specimens with a diameter of 10 mm and a thickness of 2 mm were cut from the round rod using the diamond saw. For Zr, square plates with a thickness of 2 mm and an edge length of 10 mm were cut out of the blank using the diamond saw, and which were subsequently sintered at 1500°C for 24 hours in a ceramic furnace (Thermo Star, Thermo-Star GmbH, Aachen, Germany; Figure 6).



Figure 6: The ceramic furnace (Thermo Star, Thermo-Star GmbH, Aachen, Germany) used for sintering the Zr samples.

Afterwards, all specimens were subjected to surface polishing, using a standardized procedure with 800, 1200, 2500, and 4000 grit rotating silica carbide (SiC) papers (Hermes Schleifmittel GmbH, Hamburg, Germany) under water cooling with a polishing machine (Exakt 400 CS, EXAKT Advanced Technologies GmbH, Norderstedt, Germany; Figure 7).



Figure 7: The polishing machine (Exakt 400 CS, EXAKT Advanced Technologies GmbH, Norderstedt, Germany) used to polish the sample surfaces.

2.2 Surface characterization.

2.2.1 Surface Roughness

Surface roughness (R_a) was determined on the surface of all samples using the Alicona infinite focus system (Alicona Imaging GmbH, Raaba/Graz, Austria). 3D scans of each of 5 separate areas of the surfaces were taken at 10-fold magnification. On each of these scans, 4 lines were drawn in a zigzag arrangement with a total length of 4 mm, by which the R_a value was then determined (Figure 8).

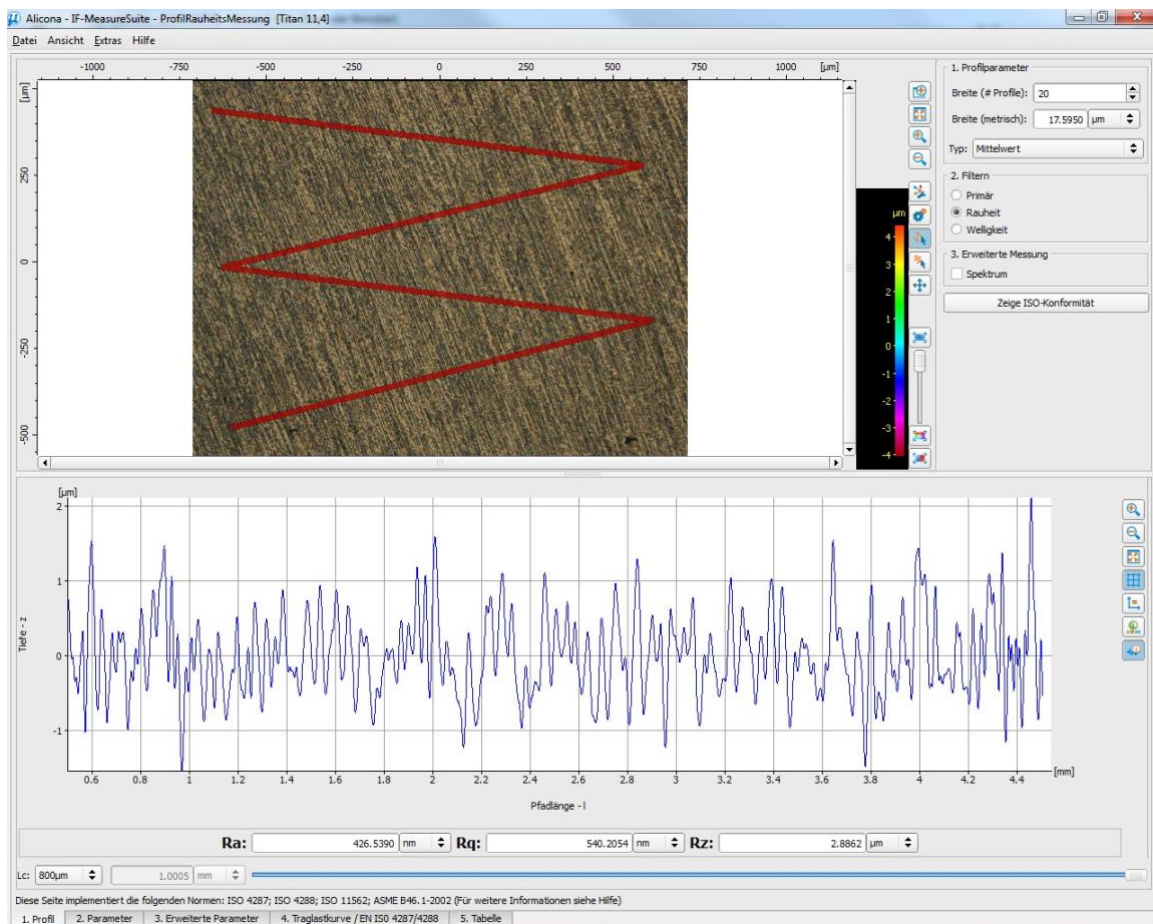


Figure 8: Procedure of the surface roughness measurement using the Alicona infinite focus system (Alicona Imaging GmbH, Raaba/Graz, Austria).

2.2.2 Contact Angle

To evaluate the surface wettability, the water contact angle was measured with the sessile drop method using a digital microscope (Keyence VHX-5000, Keyence GmbH, Neu-Isenburg, Germany).

A 20- μl water droplet was put on the surface of the samples at room temperature. After 10s, a picture was taken and the contact angles of each side of the droplet were measured and averaged (Figure 9).

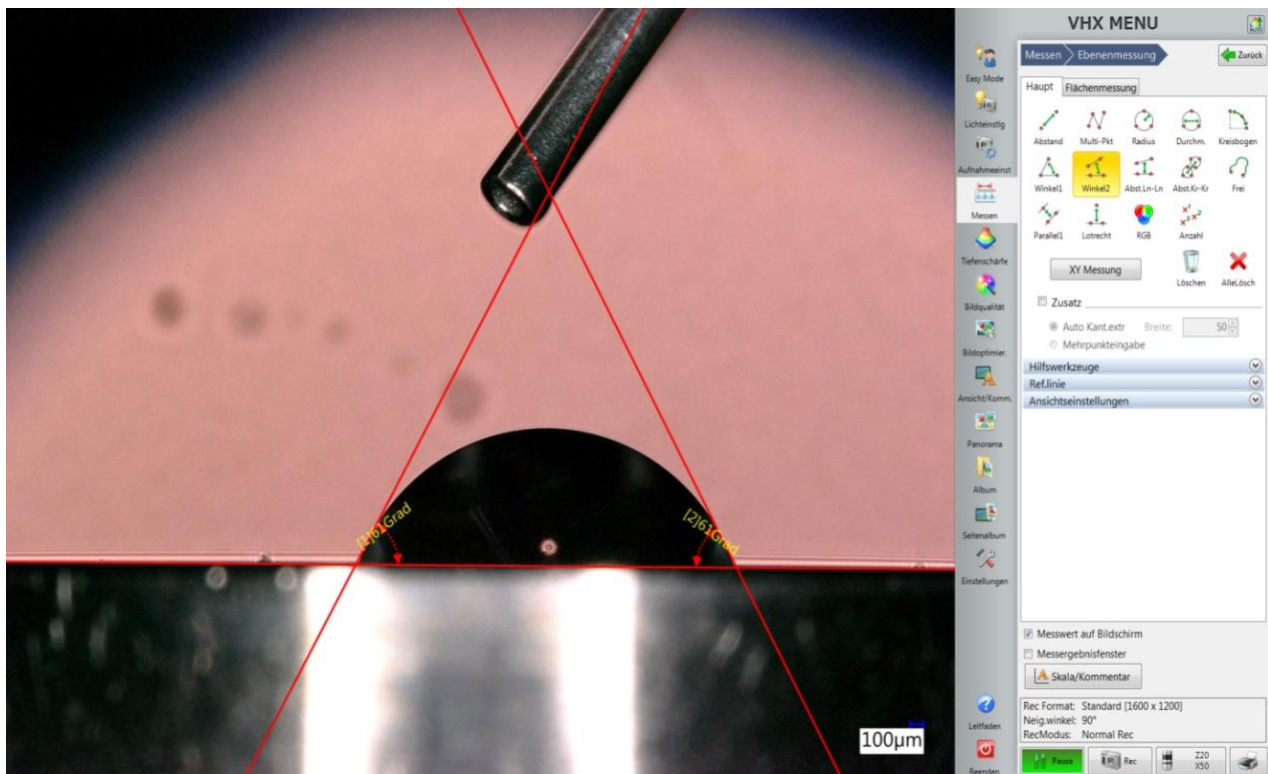


Figure 9: Exemplary contact angle measurement.

2.3 Microbiological culture.

Tryptic soy broth (TSB) was prepared by combining the following ingredients:

- trypticase soy broth (6 g)
- yeast extract (0.6 g)
- sterile distilled water (200 ml).

The ingredients were carefully measured using a precision scale (BP 221 S, Sartorius, Göttingen, Germany), and mixed in a 1-liter laboratory bottle. The broth was sterilized afterwards in the microwave until boiling. The bottle was then removed from the microwave and closed 2 minutes later. After 2 hours, the sterilization procedure was repeated. Later, the TSB medium was stored in the refrigerator at 2 °C until the day of the experiment.

Streptococcus sanguinis (DSM 20068) and agar plates were kindly provided by the department of periodontology of the Charité-University Medicine Berlin.

The bacteria were incubated on the agar plates for 1 to 2 days in a 5 % CO₂ atmosphere to obtain single colonies.

After 1-2 days of incubation, the bacterial colonies were collected by scraping from the agar plate and thoroughly mixed into a matching amount of TSB medium within a 50 ml centrifuge tube (Falcon, Fisher Scientific GmbH, Schwerte, Germany). The tube was put on a circle shaker (KS 260 basic, IKA, Germany) and incubated at 37 °C at 40 rpm overnight. After 24 h the bacterial suspension could then be transferred to the experimental part of the study.

The samples were washed with 60 % alcohol, put into 24-well plates and again covered with 60 % alcohol for 30 minutes. The samples were then washed twice with sterile water and put into a new 24-well plate.

In order to obtain a specific concentration of the bacteria in the medium, the optical density at wavelength 600 nm (OD₆₀₀) was adjusted to ca. 0.5 using a photometer (BioPhotometer Plus, Eppendorf AG, Hamburg, Germany; *Figure 10*) by comparing 500 µl TSB medium to 500 µl bacterial suspension, to which a calculated amount of TBS medium was added (diluting the bacterial suspension) until the optical density level of 0.5 was reached. Each measurement was repeated three times.

Afterwards, 1000 μl of the bacterial suspension was added to each sample. The samples in the 24-well plates were then incubated for 3 hours on the circle shaker at 37 $^{\circ}\text{C}$ and 40 rpm in a 5 % CO_2 atmosphere.



Figure 10: The photometer (BioPhotometer Plus, Eppendorf AG, Hamburg, Germany) which was used to obtain a bacterial concentration in the TSB medium.

After the 3 hours of incubation, the samples were carefully rinsed three times with a phosphate buffered saline (PBS) to remove debris and non-adherent bacteria from the surface and to buffer the pH value to a physiological value of 7.4.

Afterwards, the samples were put into new 24-well plates and covered with 1000 μ l TBS medium and incubated again on the circle shaker at 37°C for 18 hours.

The samples were then rinsed with the PBS again to remove debris and non-adherent bacteria, every sample was rinsed 3 times carefully and gently, and thus, the samples were ready to be scanned using the microscope.

2.4 Fluorescence microscopy of bacterial colonies

Principles of fluorescence microscopy

Fluorescence is the emission of light from objects which have absorbed light in a specific wavelength and exhausted it again in a different wavelength within nanoseconds. The difference between these wavelengths can be visualized with a fluorescence microscope via a different spectral color. The ability of these objects to be fluorescent is related to their physical and chemical properties, so some objects are auto fluorescent and some are not. For auto fluorescent objects, the way in which they absorb light and their power of light emission differs, so the molecules that have good auto fluorescent properties are used as detectors for other materials which have a lower fluorescence ability, and are called fluorophores (78).

As the fluorophore, FDA (fluorescein diacetate) was chosen to stain the viable bacteria since it showed the best results in the frame of the preliminary tests.

Using blue light with a wavelength of 450 nm, FDA causes a bright yellow-green emitted light with a wavelength about 550 nm after reacting with the cell under the fluorescence microscope (Figure 11 and 12).

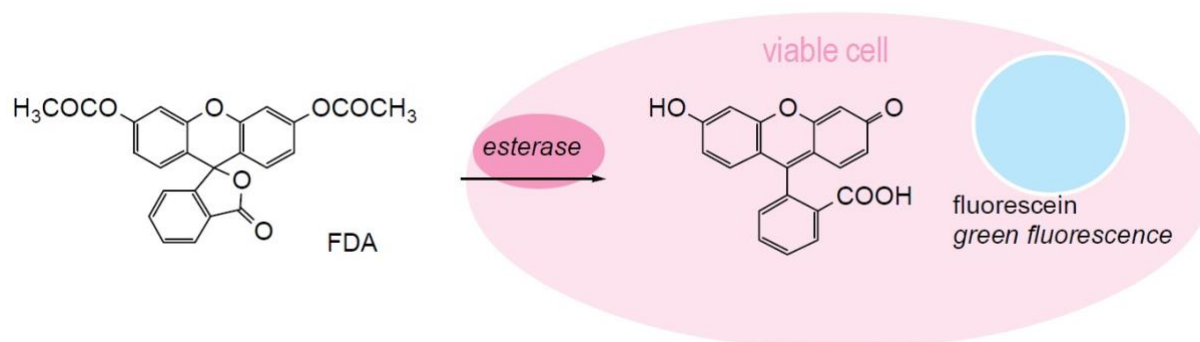
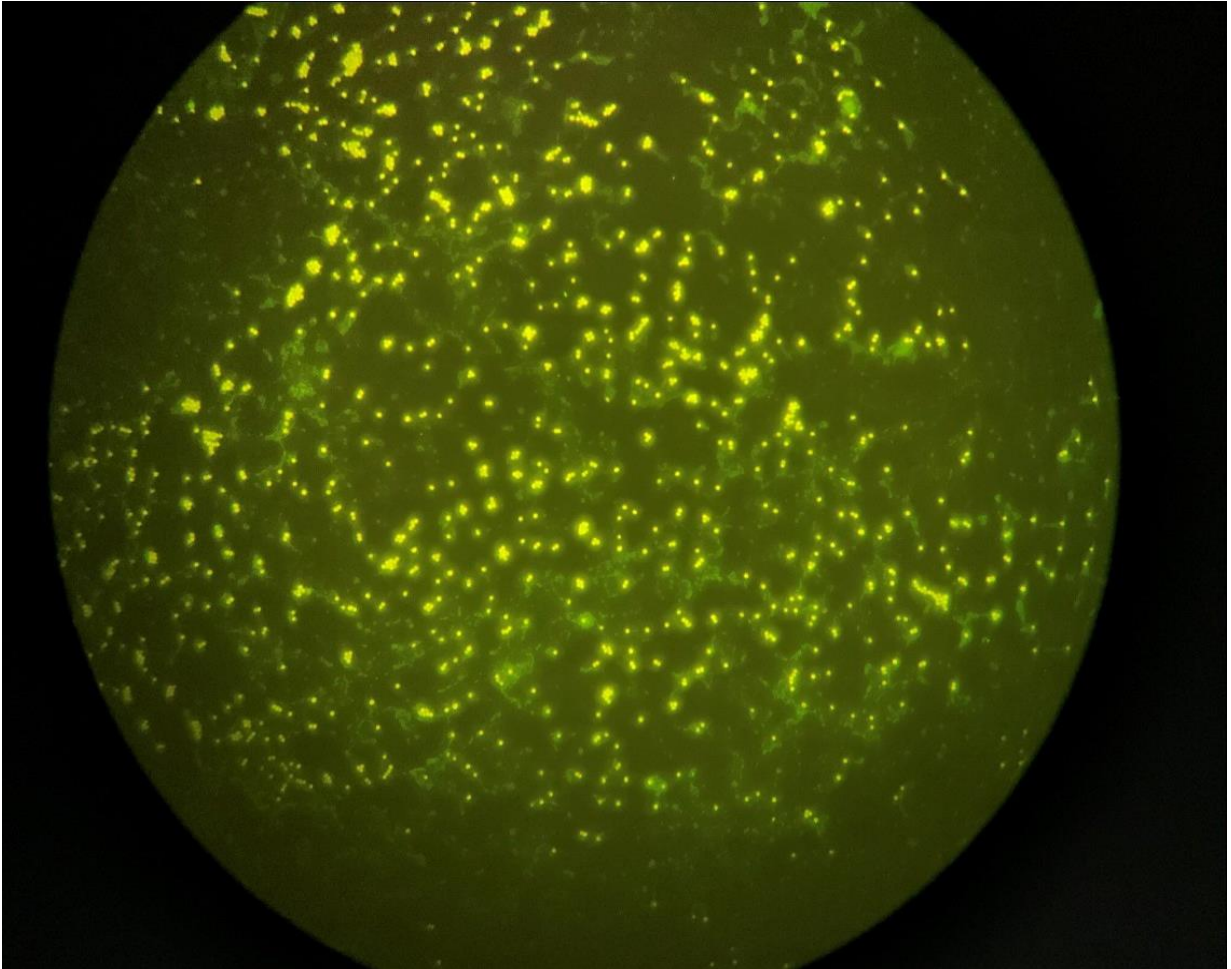


Figure 11: The cell staining mechanism using FDA.

(The image was taken from https://www.dojindo.eu.com/Images/Product%20Photo/F209_fig1.jpg).

A 5 mg/ml FDA stock solution was stored at -20° in the dark until usage. For usage, it was diluted in PBS in a ratio of 1:100 and covered with aluminum foil due to its light sensitivity. From this solution, 1000 μ l was added to each sample in the well plates. The well plates were covered with aluminum foil and incubated at 37°C for 30 minutes.



*Figure 12: Fluorescence microscopic image of *S. sanguinis* colonies after incubation with FDA for 30 minutes.*

For every specimen, three pictures of different rectangular (2.5 mm X 2.0 mm) areas (right, middle, left) of the surface were taken using a fluorescence microscope (Vanox T AH-2 DIC, OLYMPUS EUROPA SE & CO. KG, Hamburg, Germany; Figure 13) with an exposure time of 100 ms at 5x magnification using blue light with a wavelength of 450 nm, with a total of 180 pictures of all the specimens in this study.



*Figure 13 : The fluorescence microscope (Vanox T AH-2 DIC, OLYMPUS EUROPA SE & CO. KG, Hamburg, Germany), which was used to visualize the *S. sanguinis* colonies after 18 hours of incubation.*

The pictures were then modified using Photoshop version 14 (Adobe Inc., California, USA) to make the adherent colonies visible.

Preliminary tests showed that the strong intrinsic fluorescence of PEEK, which makes it impossible to visualize and detect the colonies, could be circumvented by adjusting the brightness and contrast of the images. For this, a specific filter in Photoshop called "Curves" was used. All the pictures, including the ones of Zr and Ti, were processed with the same filter to ensure a standardized procedure (Figure 14).

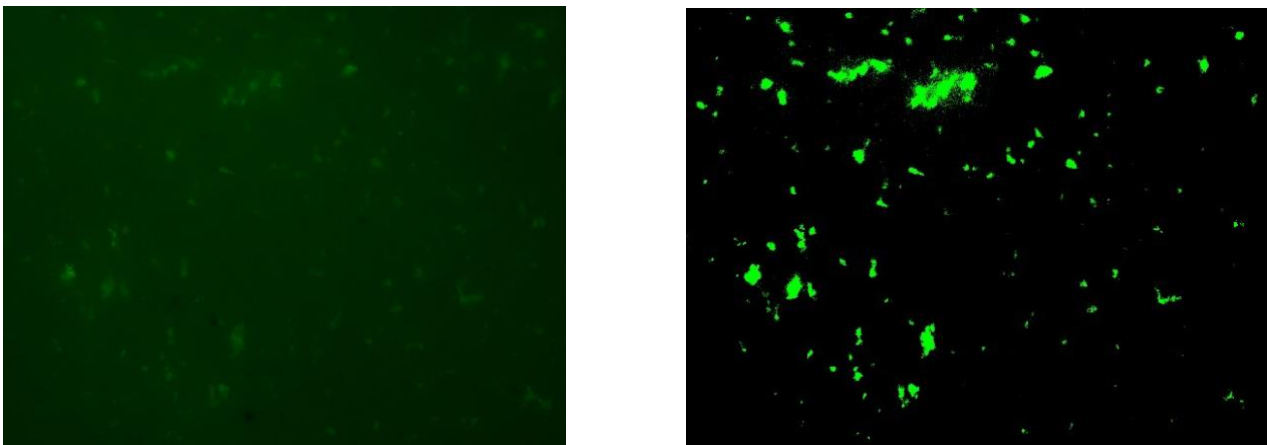


*Figure 14: Fluorescence microscopic images of *S. sanguinis* colonies on W-PEEK incubated with FDA for 30 minutes, before editing (left) and after editing (right).*

Afterwards the colonies were counted using Image J 1.53i (Figure 15), whereby a minimum area of 100-1000 pixels and circularity of 0.00-1.00 was considered a colony.

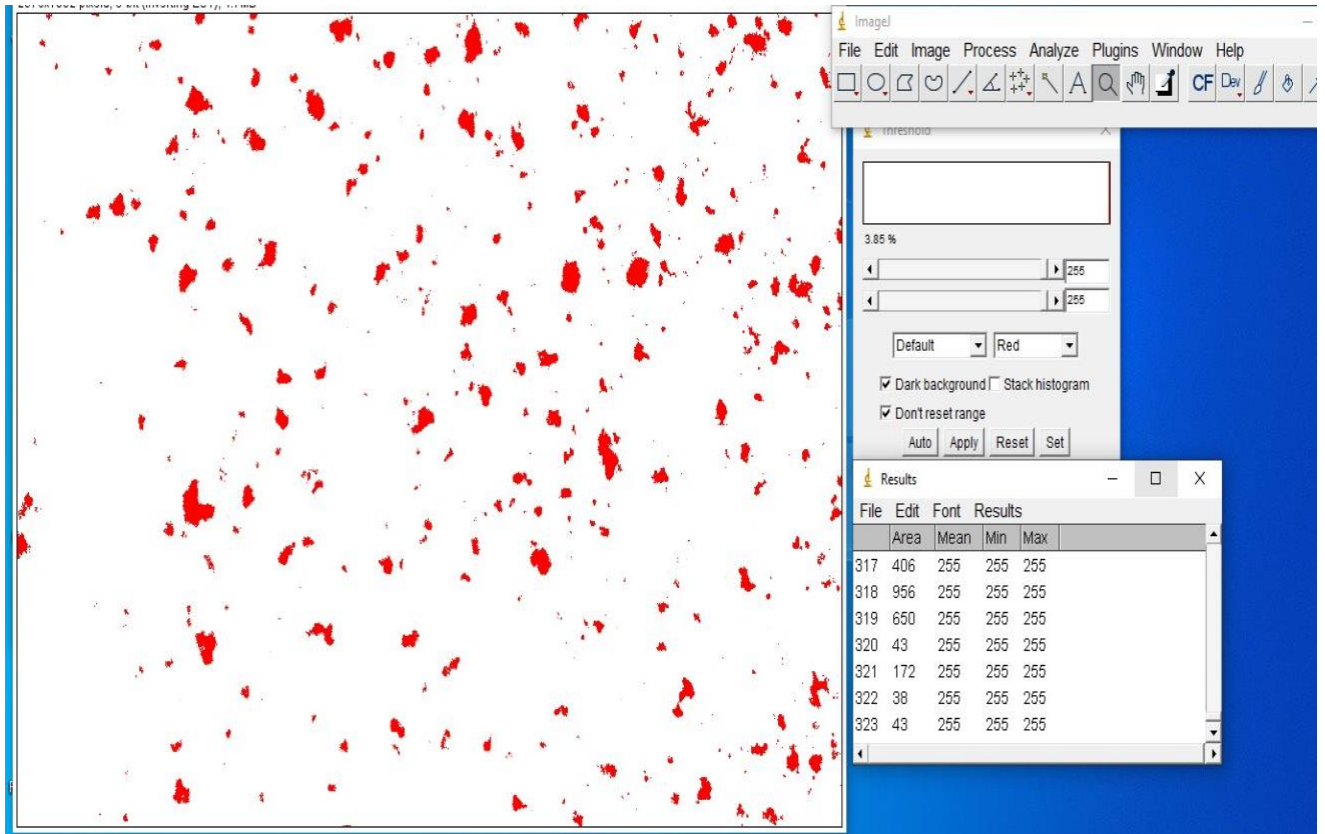


Figure 15: Due to the image processing in ImageJ, the colonies on the fluorescence images (here on W-PEEK) show as red areas, which are counted by the software.

2.5. Statistical analysis:

Statistically significant differences between groups were analyzed by one-way ANOVA and Tukey's multiple comparison tests.

The contact angle measurement, the surface roughness measurement and the biofilm measurement were carried out using the one-way ANOVA, followed by the Tukey's post hoc test.

The statistical significance was evaluated using SPSS 27.0 software (SPSS IBM, Chicago, IL, USA).

A p value <0.05 was considered statistically significant.

3. RESULTS

3.1 Surface characterization

3.1.1 Surface Roughness measurements

Table 2 shows the mean surface roughness of the different groups, which are visualized in Figure 16.

Table 2: Summary of the surface roughness (Ra) of the different groups (mean \pm SD).

Groups	Ra [μm]
W-PEEK	0.61 ± 0.08
R-PEEK	0.66 ± 0.08
B-PEEK	0.61 ± 0.12
P-PEEK	0.55 ± 0.11
Zr	0.54 ± 0.05
Ti	0.43 ± 0.09

One-way ANOVA indicated a significant difference in the surface roughness between the W-, B- and P-PEEK from one side, and the R-PEEK, Zr and Ti from the other side ($P < 0.05$).

Titanium showed the smoothest surface, with an average of $0.43 \pm 0.09 \mu\text{m}$. This result was significantly different to W-PEEK, R-PEEK and B-PEEK ($P < 0.05$).

Zirconium dioxide showed the second smoothest surface, with an average of $0.54 \pm 0.05 \mu\text{m}$, which was not significantly different to the other groups.

P-PEEK showed a rougher surface compared to titanium and zirconium dioxide, and was smoothest of the PEEK groups, with a mean value of $0.55 \pm 0.11 \mu\text{m}$, which was not significantly different to the other groups.

R-PEEK had the roughest surface, with a mean Ra value of $0.66 \pm 0.08 \mu\text{m}$. The other PEEK materials showed slightly smoother surfaces, with a mean Ra of $0.61 \pm 0.12 \mu\text{m}$ for B-PEEK and an average of $0.61 \pm 0.08 \mu\text{m}$ for W-PEEK.

Results

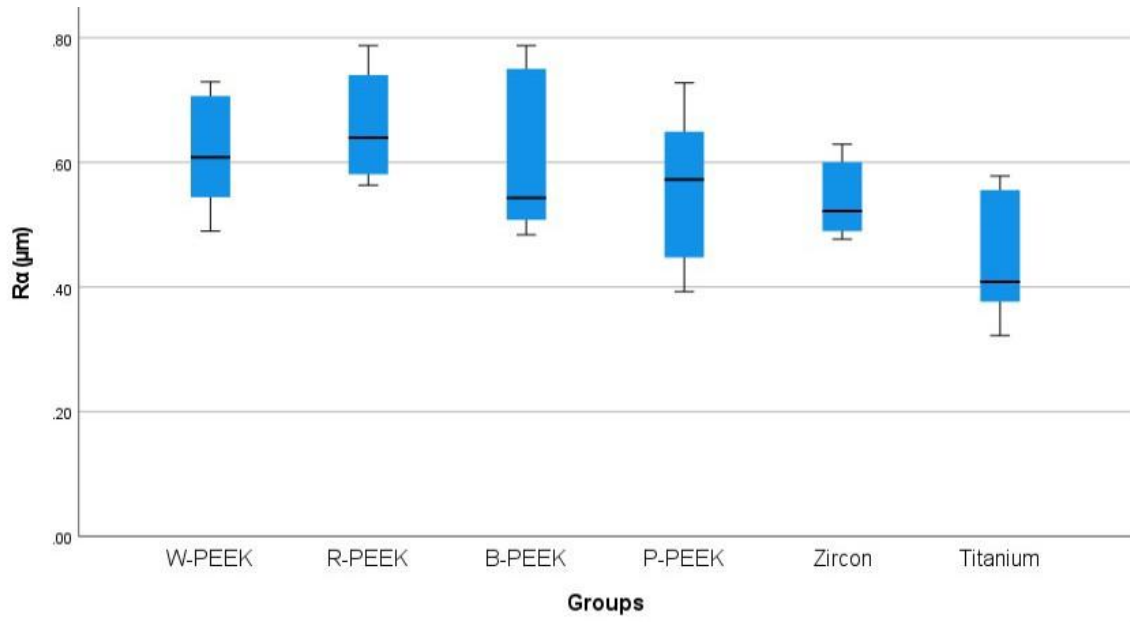
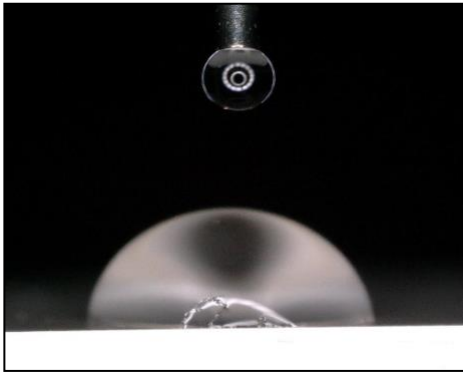


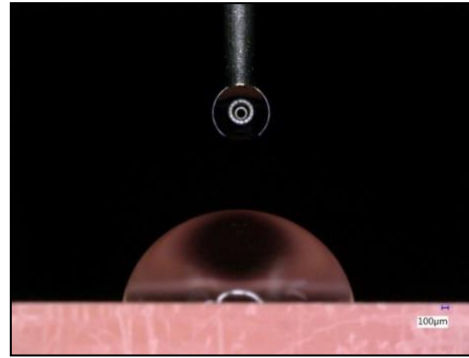
Figure 16: Boxplot of the surface roughness of the different groups.

3.1.2 Contact Angle measurements

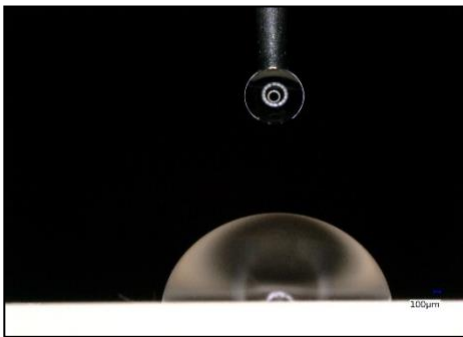
Figure 17 shows one image of each group after application of the water droplet to measure the contact angle.



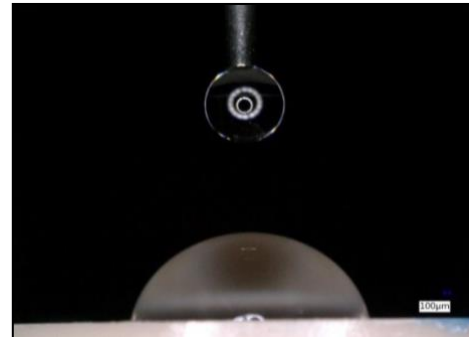
W-PEEK



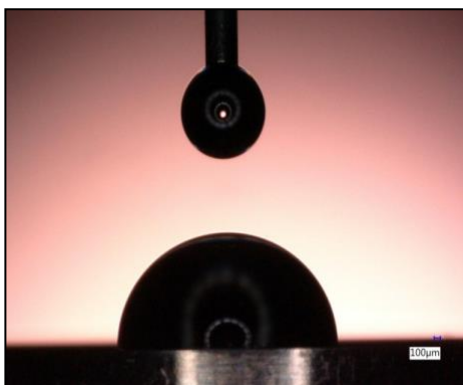
R-PEEK



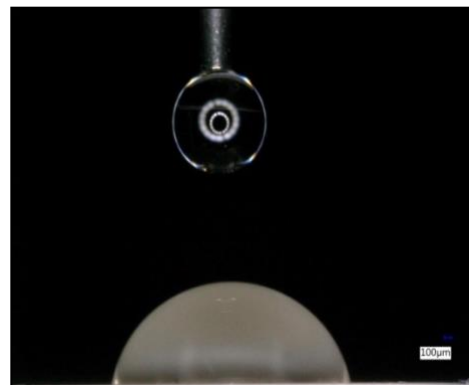
B-PEEK



P-PEEK



Ti



Zr

Figure 17: Exemplary water contact angles of the different groups.

Table 3 summarizes the mean water contact angles, which are visualized in Figure 18.

Table 3: Summary of the water contact angle measurements of the different groups (mean \pm SD).

Group	Water contact angle (°)
W-PEEK	71 \pm 3.73
R-PEEK	72 \pm 2.92
B-PEEK	72.48 \pm 3.48
P-PEEK	66.65 \pm 9.26
Zr	66.26 \pm 9.39
Ti	71.75 \pm 6.56

There was no significant difference between the results of the water contact angles of the different groups.

B-PEEK, with an average $72.48 \pm 3.48^\circ$ in water contact angle was the most hydrophobic material, comparable to R-PEEK with an average of $72 \pm 2.92^\circ$, W-PEEK ($71 \pm 3.73^\circ$) and Ti ($71.75 \pm 6.56^\circ$) without significant differences.

Zr and P-PEEK showed the most hydrophilic surfaces, with a mean water contact angle of $66.26 \pm 9.39^\circ$ and $66.65 \pm 9.26^\circ$, respectively.

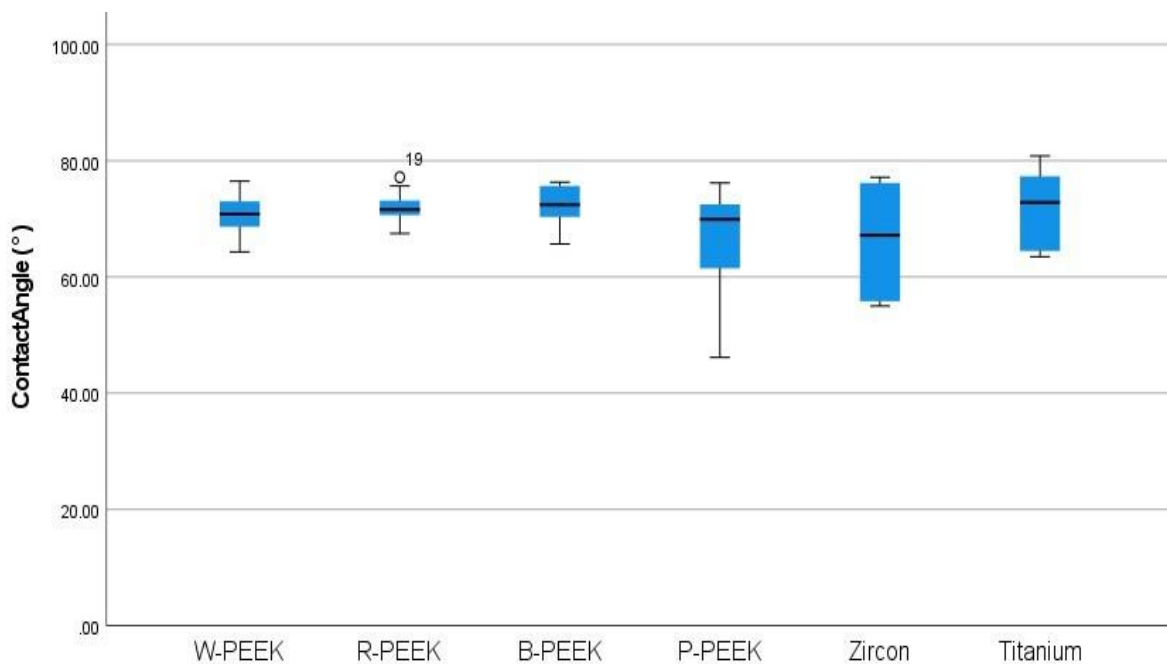


Figure 18: Boxplot of the water contact angles of the different groups.

3.2. Biofilm Formation

Figure 19 shows fluorescence microscopic images of the biofilm formation on the surfaces of the different materials before and after editing.

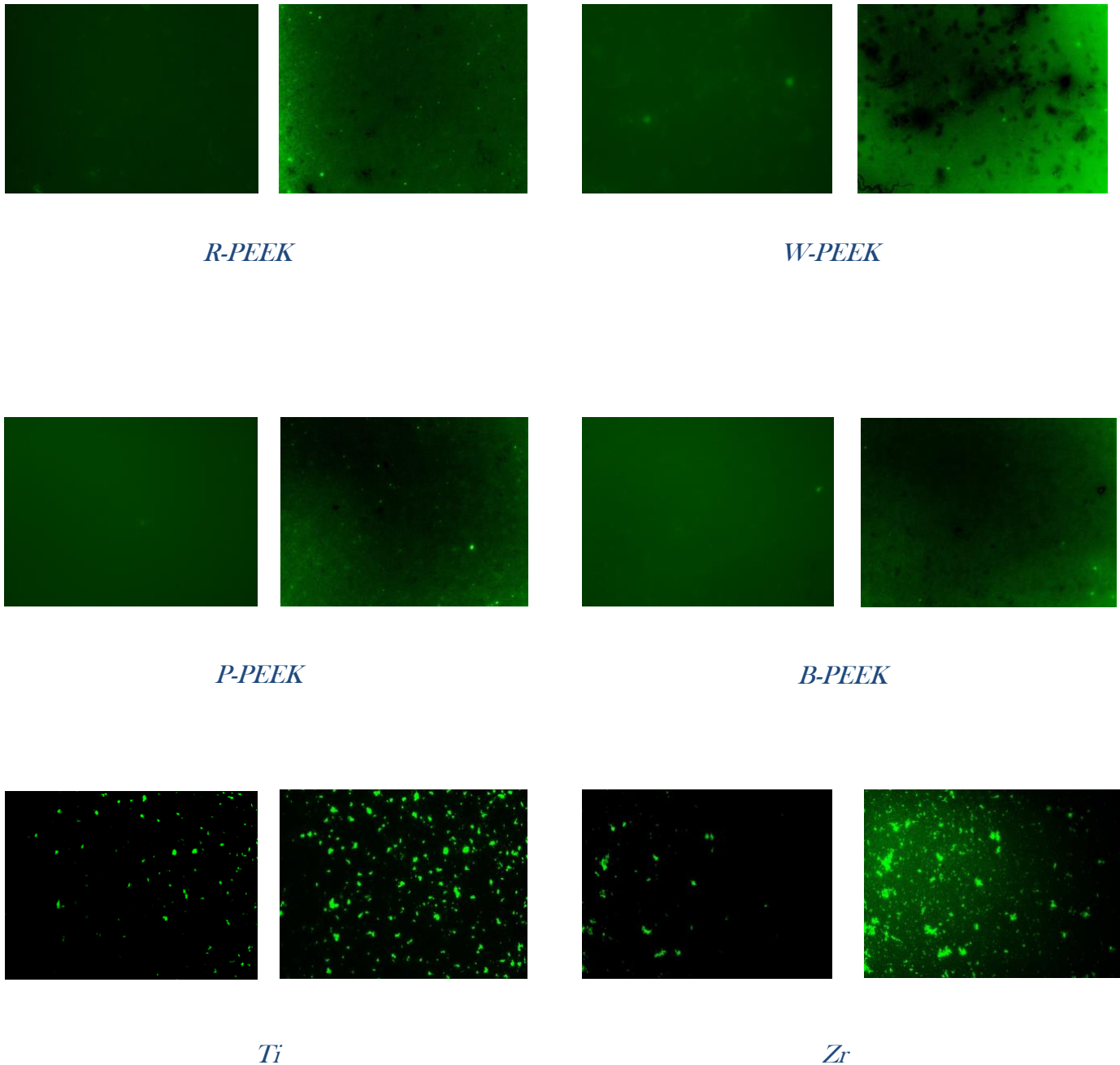


Figure 19: Exemplary fluorescence microscopic images of the different groups after 18 hours of incubation of *S. sanguinis* colonies, before (left) and after editing (right).

Results

Table 4 summarizes the number of adherent colonies of *S. sanguinis* on the surfaces of the different groups, while the results are visualized in Figure 20.

Table 4: Summary of the adherent colonies on the surfaces of the different groups.

Group	Number of adherent colonies (mean \pm SD)
W-PEEK	32.43 \pm 29.65
B-PEEK	15.63 \pm 7.51
R-PEEK	96.1 \pm 39.01
P-PEEK	22.56 \pm 33.90
Zr	100.7 \pm 37.01
Ti	108.2 \pm 49.42

Results

After 18 hours of incubation, the lowest amount of adherent viable biomass of *Streptococcus sanguinis* was identified on the surface of B-PEEK (15.63 ± 7.51 colonies), which was significantly lower than Zr (100.7 ± 37.01 colonies), R-PEEK (96.1 ± 39.01 colonies) and Ti (108.2 ± 49.42 colonies).

P-PEEK, with an average of 22.56 ± 33.90 colonies, showed the second lowest number of colonies, with a non-significant difference to B-PEEK and W-PEEK (32.43 ± 29.65 colonies), but with a significant difference compared to Zr, R-PEEK and Ti ($P < 0.05$). W-PEEK showed the third lowest number of colonies, with a significant difference to Zr, R-PEEK and Ti ($p < 0.05$).

Of the PEEK groups, R-PEEK showed the highest number of colonies, which was significantly different to the other PEEK groups ($P < 0.05$), whereas the mean number of colonies on R-PEEK was not significantly lower than the ones of Ti and Zr.

Ti showed the highest number of adherent colonies from *Streptococcus sanguinis*, which was significantly higher than the number of colonies on W-PEEK, B-PEEK and P-PEEK.

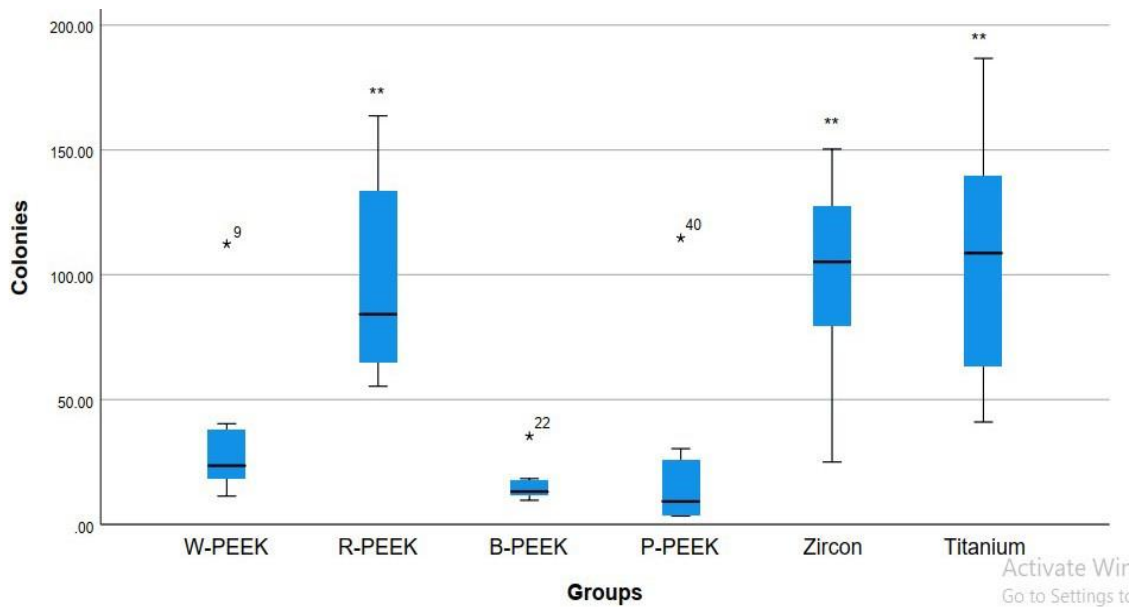


Figure 20: Boxplot of the number of adherent colonies of the different groups. (**) significantly different to W-, B- and P-PEEK.

4. Discussion

The aim of this *in vitro* study was to investigate the biofilm formation of an early colonizer species (*S. sanguinis*) on the surfaces of different types of PEEK materials, with Titanium and zirconia serving as controls.

The bacterial growth differed significantly between R-PEEK, Ti and Zr, on the one hand, and W-PEEK, B-PEEK and P-PEEK on the other hand. This could have been caused by different reasons, including the surface roughness. This could have been the reason in the case of R-PEEK, since it showed the highest surface roughness. In general, the topography of a surface can affect bacterial adhesion (79,80), whereas a high surface roughness enhances bacterial adhesion and growth (81).

In case of Zr, the high number of colonies could be attributed to its high wettability based on its low contact angle, since a high hydrophilicity can also enhance bacterial adhesion (82), resulting in a positive correlation between the hydrophilicity of a material and the number of adherent bacterial colonies on its surface (83).

In case of titanium, the high number of colonies could not be attributed to its surface roughness, since Ti showed the smoothest surface. Moreover, titanium did not show the lowest contact angle, so the reason for the high number of adherent bacterial colonies was not obvious.

Taking this into account, as well as the low numbers of adherent colonies on W-, B- and P-PEEK, despite their surface roughness being similar to that of R-PEEK, the results of the present study do not agree with the results of previous studies, where an increase in the surface roughness led to an increase in the number of bacterial colonies in the biofilm in comparison with smoother surfaces (83). However, when looking at the PEEK materials separately, the results were in accordance with the studies, whereby the surface roughness correlated with the numbers of adherent colonies, since R-PEEK showed the highest surface roughness and highest number of adherent bacterial colonies compared to the other PEEK materials of the P-, W-, and B-PEEK groups.

Discussion

Besides the surface roughness and wettability, the chemical composition of a material may play an additional important role in biofilm formation (84). According to Scheuerman et al., the attachment of bacteria to different surfaces involves complex mechanisms with different chemophysical forces that will either attract or repel bacteria (85).

In contrast to P-PEEK, the other PEEK grades contain pigment powders, such as TiO₂ in the case of W-PEEK, so as to adapt their intrinsic color to the specific field of application. Whether these powders could have had a negative influence on the polishability, and thus have had an indirect or a direct influence on the bacterial adhesion due to their material properties, would need to be clarified in the future.

The results of the present study are in accordance with the literature, where titanium shows a high contact angle in combination with a high number of adherent colonies (83).

Despite the low contact angle, P-PEEK showed a very low number of adherent bacteria. This could have probably been caused by its surface roughness, so that air could have been trapped in the surface irregularities, repelling the bacteria (81).

Preliminary studies showed that the PEEK materials included in this study were difficult to evaluate under the fluorescence microscope due to their intrinsic fluorescence. Therefore, various detectors had to be tested due to the strong light reflection of PEEK, such as methylene blue as a standard dye, and later fluorophores such as DAPI (4',6-diamidino-2-phenylindole), FITC (fluorescein isothiocyanate) and FDA (fluorescein diacetate).

Additionally, the microscopic images had to be edited to make the colonies visible. This procedure was carried out carefully in order to avoid leaving any colonies undetected, which could not be guaranteed completely.

Furthermore, it could not be guaranteed that all relevant colonies were detected, since fluorochrome FDA only makes living bacteria visible (86). Therefore, after the incubation with FDA, the surfaces were scanned immediately to avoid any delay. However, the additional detection of the dead bacteria adhering to the surfaces would be also of high interest. Moreover, other possible fluorochromes sensitive to other light spectra should be evaluated in the future, in order to avoid the intrinsic fluorescence of PEEK.

Biofilm formation in the oral cavity is a very complicated process, and still not completely clarified yet. This study was based on an attempt to create a simplified *in vitro* test setup to provide an indication of the plaque affinity of the tested materials. Therefore, *S. sanguinis* was

Discussion

used, since it is considered to be crucial for plaque formation, due to its role as one of the early colonizers. This *in vitro* study showed that *S. sanguinis* has the ability to adhere to the surface of different PEEK materials as well as to the other implant materials titanium and zirconia, despite the absence of the acquired pellicle, which may be due to its special properties as an early colonizer (87). These results were similar to other studies which investigated the growth of bacteria (*Staphylococcus epidermidis*, *Pseudomonas aeruginosa*, and *Escherichia coli*) on different orthopedic polymers (PEEK was one of them) (88). However, *in vivo*, namely in the oral cavity, there are more than 700 types of bacteria which are also important for biofilm formation, especially if they interact with each other. As mentioned above, another important factor for biofilm formation is the acquired pellicle, which consists of several proteins. These proteins have an influence on bacterial adherence, in that they can prevent and enable bacteria to adhere at the same time. Due to the absence of other bacteria and the acquired pellicle, the present *in vitro* results could differ significantly from *in vivo* results (89). Another limitation of the study could have been the low number of specimens of n=10 per group.

The interface between the oral tissues and implant materials has always been of great interest so as to better understand osseointegration on the one hand, and the mechanism of bacterial colonization on the other, as well as to be able to minimize the cumulative results such as inflammatory diseases and implant failure, and to maintain healthy conditions to achieve higher success rates by improving the techniques and materials used in dental implantology (90). Therefore, with the introduction of new materials such as PEEK, new challenges have arisen in the field of dentistry.

5. Conclusion

Within the limits of this *in vitro* study, three different PEEK compounds - including a pure implantable PEEK grade - showed the least bacterial adhesion, while titanium showed the highest, followed by zirconium dioxide and another red dental PEEK grade, using *S. sanguinis* as an early colonizer within the biofilm formation process.

In vivo investigations are needed to establish whether these results can be used to make a statement regarding the plaque affinity of the investigated materials, and also to prove whether the test setup used could be used for the examination of other materials.

6. References

1. Dewhirst FE, Chen T, Izard J. The human oral microbiome. *J Bacteriol.* **2010**; 192:5002-5017.
2. Abranches J, Zeng L, Kajfasz JK, Palmer SR, Chakraborty B, Wen ZT, Richards VP, Brady IJ, Lemos JA. Biology of Oral Streptococci. *Microbiol Spectr.* **2018**.
3. Kolenbrander PE, Palmer RJ Jr, Rickard AH, Jakubovics NS, Chalmers NI, Diaz PI. Bacterial interactions and successions during plaque development. *Periodontol 2000* **42** (2006) 47-79.
4. Slots J. Periodontitis: facts, fallacies and the future. *Periodontol 2000.* **2017** Oct;75(1):7-23.
5. Nyvad B, Kilian M: Microbiology of the early colonization of human enamel and root surfaces *in vivo*. *Scand J Dent Res.* **1987**, *95*: 369-380.
6. Schwarz F, Derks J, Monje A, Wang H. L. Peri-implantitis. *J Periodontol* **89** (2018) S267-90.
7. Jung RE, Pjetursson BE, Glauser R, Zembic A, Zwahlen M, Lang NP. A systematic review of the 5-year survival and complication rates of implant-supported single crowns. *Clin Oral Implants Res.* **2008**; 19:119-130.
8. Papia E, Larsson C. Material-related complications in implant-supported fixed dental restorations. A systematic review. *Eur J Oral Implantol.* **2018**;11 Suppl 1:S147-S165.
9. Bassetti RG, Bassetti MA, Kuttenger J. Implant-Assisted Removable Partial Denture Prosthesis: A Critical Review of Selected Literature. *Int J Prosthodont.* **2018** May/Jun;31(3):287-302.

10. Ottria L, Lauritano D, Andreasi Bassi M, Palmieri A, Candotto V, Tagliabue A, Tettamanti L. Mechanical, chemical and biological aspects of titanium and titanium alloys in implant dentistry. *J Biol Regul Homeost Agents*. 2018 Jan- Feb;32(2 Suppl. 1):81-90.
11. Parmigiani-Izquierdo JM, Cabaña-Muñoz ME, Merino JJ, Sánchez-Pérez A. Zirconia implants and peek restorations for the replacement of upper molars. *Int J Implant Dent*. 2017 Dec;3(1):5.
12. Gupta R, Gupta N, Weber KK. Dental Implants. 2021 Aug 11. In: StatPearls.
13. S. Najeeb, M.S. Zafar, Z. Khurshid, F. Siddiqui, Applications of polyetheretherketone (PEEK) in oral implantology and prosthodontics, *J. Prosthodont. Res.* 60 (2016) 12-19.
14. Kurtz SM, Devine JN. PEEK biomaterials in trauma, orthopedic, and spinal implants. *Biomaterials*. 2007 Nov;28(32):4845-69.
15. Zoidis P, Bakiri E, Papathanasiou I, Zappi A. Modified PEEK as an alternative crown framework material for weak abutment teeth: a case report. *Gen Dent*. 2017;65(5):37-40.
16. M.R Tant, H.L.N. McManus, M.E. Rogers, High-temperature properties and applications of polymeric materials, in: M.R Tant, H.L.N. McManus, M.E. Rogers (Eds.), ACS Symposium Series, ACS, 1995, pp. 1-20.
17. Stoodley P, Sauer K, Davies DG, Costerton JW. Biofilms as complex differentiated communities. *Annu Rev Microbiol* 2002; 56:187-209.
18. Lang NP, Berglundh T; Working Group 4 of Seventh European Workshop on Periodontology. Periimplant diseases: where are we now? --Consensus of the Seventh European Workshop on Periodontology. *J Clin Periodontol*. 2011 Mar;38 Suppl 11:178-81.
19. GBD 2017 Disease and Injury Incidence and Prevalence Collaborators. Global, regional, and national incidence, prevalence, and years lived with disability for 354 diseases and injuries for 195 countries and territories, 1990-2017: a systematic analysis for the Global Burden of Disease Study 2017. *Lancet*. 2018 Nov 10;392(10159):1789-1858.

20. Hojo. K. Nagaoka. S. Ohshima. T. & Maeda. N. (2009). Bacterial interactions in dental biofilm development. *Journal of Dental Research*. 88(11). 982-990.
21. Lockhart PB, Brennan MT, Sasser HC, Fox PC, Paster BJ, Bahrani-Mougeot FK. Bacteremia associated with toothbrushing and dental extraction. *Circulation*. 2008;117(24):3118-3125.
22. Vitorino R, Lobo MJC, Ferrer-Corriera AJ, Dublin JR, Tomer KB, Domingues PM, Amado FML: Identification of human whole saliva protein components using proteomics. *Proteomics* 2004, 4:1109-1115.
23. Kolenbrander PE. Oral microbial communities: Biofilms. interactions. and genetic systems. *Annu Rev Microbiol* 2000; 54: 413-437.
24. Gibbons RJ, Van Houte J. On the formation of dental plaques. *J Periodontol*. 1973; 44:347-60.
25. Lindhe J. editor. 4th ed. Oxford. UK: Blackwell Publishing Company; 1998. *Clinical Periodontology and implant dentistry book*. Chapter 3, 84-97.
26. Furst MM, Salvi GE, Lang NP. Bacterial colonization immediately after installation of oral titanium implants. *Clin Oral Implants Res*. 2007; 18:501-8.
27. Kalykakis GK, Nissengard R. Clinical and microbial findings on osseointegrated implants, comparison between partially dentate and edentulous subjects. *European J Prosthodont Rest Dent*. 1998; 6:155-9.
28. Arciola C.R., Campoccia D., Speziale P., Montanaro L., Costerton J.W., Biofilm formation in Staphylococcus implant infections. A review of molecular mechanisms and implications for biofilm resistant materials. *Biomaterials* 2012; 33:5967-82.
29. Ata-Ali J., Candel-Martí M.E., Flichy-Fernández A.J., Penarrocha-Oltra D., Balaguer-Martínez J.F., Penarrocha Diago M., Peri-implantitis: Associated microbiota and treatment. *Med Oral Patol Oral Cir Bucal* 2011;16: e937-43.

30. Shibli J.A., Melo L., Ferrari D.S., Figueiredo L.C., Faveri M., Feres M., Composition of supra-and subgingival biofilm of subjects with healthy and diseased implants. *Clinical oral implants research* **2008**; 19:975-82.
31. Mombelli A, Lang NP, Microbial aspects of implant dentistry. *Periodontology* **2000**. 1994;74-80.
32. Paquette DW, Brodala N, Williams RC. Risk factors for endosseous dental implant failure. *Dent Clin North Am.* **2006**; 50:361-74.
33. Roos-Jansåker AM, Renvert H, Lindahl C, Renvert S. Nine- to fourteen-year follow-up of implant treatment. Part III: factors associated with peri-implant lesions. *J Clin Periodontol.* **2006**; 33:296-301.
34. Derks J, Tomasi C. Peri-implant health and disease. A systematic review of current epidemiology. *J Clin Periodontol.* **2015**;42(Supp1 16): S158-71.
35. Pontoriero R, Tonelli MP, Carnevale G, Mombelli A, Nyman SR, Lang NP. Experimentally induced peri-implant mucositis. A clinical study in humans. *Clin Oral Implants Res* **5(1994)**254-9.
36. El Askary A.S., Meffert R.M., Griffin T., Why do dental implants fail? *Part II. Implant dentistry.* **1999**; 8:265-78.
37. Duske K., Jablonowski L., Koban I., Matthes R., Holtfreter B., Sckell A., et al., Cold atmospheric plasma in combination with mechanical treatment improves osteoblast growth on biofilm covered titanium discs. *Biomaterials* **2015**; 52:327-34.
38. Norowski P.A., Bumgardner J.D., Biomaterial and antibiotic strategies for peri-implantitis: A review. *Journal of Biomedical Materials Research Part B: Applied Biomaterials* **2009**; 88:530-43.
39. Kumar PS, Mason MR, Brooker MR, O'Brien K. Pyrosequencing reveals unique microbial signatures associated with healthy and failing dental implants. *J Clin Periodontol* **39 (2012)** 425-33.

40. Lee T.C. History of dental implants. in: Cranin A.N. Oral Implantology. Charles C Thomas, Springfield, IL 1970: 3-5.
41. Parr G.R., Gardner L.K., Toth R.W. Titanium: The mystery metal of implant dentistry. Dental materials aspect. *J. Prosthet. Dent.* 1985; 54:410-414.
42. Williams D.E. Implants in dental and maxillofacial surgery. *Biomaterials.* 1981; 2:133-146.
43. Lemons J.E. Dental implants biomaterials. *J. Am. Dent. Assoc.* 1990; 121:716-719.
44. Craig R.G. Restorative Dental Materials. 9th ed. C.V. Mosby; St. Louis, MO, USA: 1993. p. 169.
45. Sagomonyants K.B., Jarman-Smith M.L., Devine J.N., Aronow M.S., Gronowicz G.A. The *in vitro* response of human osteoblasts to polyetheretherketone (PEEK) substrates compared to commercially pure titanium. *Biomaterials.* 2007; 24:3115-3123.
46. Berner S., Dard M., Gottlow J., Molenberg A., Wieland M. Titanium-zirconium: A novel material for dental implants. *Eur. Cells Mater.* 2009; 17:16.
47. Brånemark P.I., Adell R., Breine U., Hansson B.O., Lindstrom J., Ohlsson A. Intraosseous anchorage of dental prostheses. I. Experimental studies. *Scand. J. Plast. Reconstr. Surg.* 1969; 3:81-100.
48. Wang R.R., Fenton A. Titanium for prosthodontic applications: A review of the literature. *Quintessence Int.* 1996; 27:401-408.
49. McCracken, M. Dental implant materials, Commercially pure titanium and titanium alloys. *J. Prothodont.* 1999, 8, 40-43.
50. Lautenschlager E.P., Monaghan P. Titanium and titanium alloys as dental materials. *Int. Dent. J.* 1993; 43:245-253.

51. Niinomi M. Mechanical properties of biomedical titanium alloys. *Mater. Sci. Eng. A.* **1998**; 243:231-236.
52. Lee W.T., Koak J.Y., Lim Y.J., Kim S.K., Kwon H.B., Kim M.J. Stress shielding and fatigue limits of poly-ether-ether-ketone dental implants. *J. Biomed. Mater. Res. B Appl. Biomater.* **2012**; 100:1044-1052.
53. Lechner J, Noumbissi S, von Baehr V. Titanium implants and silent inflammation in jawbone-a critical interplay of dissolved titanium particles and cytokines TNF- α and RANTES/CCL5 on overall health? *EPMA J.* **2018**;9(3):331-343.
54. Javed F, Al-Hezaimi K, Almas K, Romanos GE. Is titanium sensitivity associated with allergic reactions in patients with dental implants? A systematic review. *Clin Implant Dent Relat Res.* **2013** Feb;15(1):47-52.
55. Van Brakel R. Noordmans HJ. Frenken J. de Roode R. de Wit GC. Cune MS. The effect of zirconia and titanium implant abutments on light reflection of the supporting soft tissues. *Clin Oral Implants Res* **2011**; 22: 1172- 1178.
56. Norbert Cionca. Dena Hashim & Andrea Mombelli. Zirconia dental implants: where are we now. and where are we heading? *Periodontology 2000.* Vol. 73. **2017**. 241-258.
57. Denry, I.: Kelly, J.R. State of the art of zirconia for dental applications. *Dent. Mater.* **2008**, 24, 299-307.
58. Rodrigues CDS, Aurélio IL, Kaizer MDR, Zhang Y, May LG. Do thermal treatments affect the mechanical behavior of porcelain-veneered zirconia? A systematic review and meta-analysis. *Dent Mater.* **2019** May;35(5):807-817.
59. Schünemann FH, Galárraga-Vinueza ME, Magini R, Fredel M, Silva F, Souza JCM, Zhang Y, Henriques B. Zirconia surface modifications for implant dentistry. *Mater Sci Eng C Mater Biol Appl.* **2019** May; 98:1294-1305.
60. Bona AD, Pecho OE, Alessandretti R. Zirconia as a Dental Biomaterial. *Materials (Basel).* **2015** Aug 4;8(8):4978-4991.

61. Özkurt, Z.; Kazazoglu, E. Zirconia dental implants: A literature review. *J. Oral Implantol.* **2011**, *37*, 367–376.
62. Scarano A. Piattelli M. Caputi S. Favero GA. Piattelli A. Bacterial adhesion on commercially pure titanium and zirconium oxide disks: an in vivo human study. *J Periodontol.* **2004** Feb;75(2):292-6. 88.
63. Rimondini L. Cerroni L. Carrassi A. Torricelli P. Bacterial colonization of zirconia ceramic surfaces: an in vitro and in vivo study. *Int J Oral Maxillofac Implants.* **2002** Nov- Dec;17(6):793-8.
64. Dubruille JH. Viguiet E. Le Naour G. Dubruille MT. Auriol M. Le Charpentier Y. Evaluation of combinations of titanium, zirconia, and alumina implants with 2 bone fillers in the dog. *Int J Oral Maxillofac Implants.* **1999** Mar-Apr;14(2):271- 7.
65. Schultze-Mosgau S. Schliephake H. Radespiel-Tröger M. Neukam FW. Osseointegration of endodontic endosseous cones: zirconium oxide vs titanium. *Oral Surg Oral Med Oral Pathol Oral Radiol Endod.* **2000** Jan;89(1):91-8.
66. Parmigiani-Izquierdo JM. Cabaña-Muñoz ME. Merino JJ. Sánchez-Pérez A. Zirconia implants and peek restorations for the replacement of upper molars. *Int J Implant Dent.* **2017** Dec;3(1):5.
67. C Rammos, C. Cayci, J.A. Castro-Garcia, I. Feiz-Erfan, S.C. Lettieri, Patient-specific polyetheretherketone implants for repair of craniofacial defects, *J. Craniofac. Surg.* **26** (2015) 631-633.
68. Wiesli MG, Ozcan M: High-performance polymers and their potential application as medical and oral implant materials: a review. *Implant Dent* **2015**; *24*:448-457.
69. Fujihara, K.; Huang, Z.M.; Ramakrishna, S.; Satknanantham, K.; Hamada, H. Performance study of braided carbon/PEEK composite compression bone plates. *Biomaterials* **2003**, *24*, 2661–2667.

70. Be'ery-Lipperman M, Gefen A. A method of quantification of stress shielding in the proximal femur using hierarchical computational modeling. *Comput Methods Biomech Biomed Engin.* 2006 Feb;9(1):35-44.
71. Lee WT, Koak JY, Lim YJ, Kim SK, Kwon HB, Kim MJ. Stress shielding and fatigue limits of poly-ether-ether-ketone dental implants. *J Biomed Mater Res B Appl Biomater.* 2012; 100:1044-1052.
72. Zhang M, Matinlinna JP. E-glass fiber reinforced composites in dental applications. *Silicon.* 2012; 4:73-78.
73. Lied. B. Roemming. P.A. Sundseth. J & Helseth. E. (2010). Anterior cervical discectomy with fusion in patients with cervical disc degeneration: A prospective outcome study of 258 patients (181 fused with autologous bone graft and 77 fused with a PEEK cage). *BMC surgery.* 10. 10.
74. Becker, W.; Doerr, J.; Becker, B.E. A novel method for creating an optimal emergence profile adjacent to dental implants. *J. Esthet. Restor. Dent.* 2012, 24, 395-400.
75. Stawarczyk. B. Beuer. F. Wimmer. T. Jahn. D. Sener. B. Roos. M. & Schmidlin. P.R. (2013) Polyetheretherketone - a suitable material for fixed dental protheses. *Journal of Biomedical Materials Research Part B: Applied Biomaterials* 101: 1209-1216.
76. Schwitalla A, WD M.ü. PEEK dental implants: a review of the literature. *J Oral Implantol.* 2013; 39:743-749.
77. Wang M, Bhardwaj G, Webster TJ. Antibacterial properties of PEKK for orthopedic applications [published correction appears in *Int J Nanomedicine.* 2021 Jun 18; 16:4189]. *Int J Nanomedicine.* 2017; 12:6471-6476. Published 2017 Sep 5.
78. Lichtman JW, Conchello JA. Fluorescence microscopy. *Nat Methods.* 2005 Dec;2(12):910-9.
79. L.G. Harris, D.O. Meredith, L. Eschbach, R.G. Richards, Staphylococcus aureus adhesion to standard micro-rough and electropolished implant materials, *J. Mater. Sci. Mater. Med.* 18 (2007) 1151-1156.

80. K.A. Whitehead, J Verran, The effect of surface topography on the retention of microorganisms, *Food bioprod. Process.* 84 (2006) 253-359.
81. Barkarmo S, Longhorn D, Leer K, et al. Biofilm formation on polyetheretherketone and titanium surfaces. *Clin Exp Dent Res.* 2019; 5:427-437.
82. Wassmann, T., Kreis, S., Behr, M., & Buegers, R. (2017). The influence of surface texture and wettability on initial bacterial adhesion on titanium and zirconium oxide dental implants. *International Journal of Implant Dentistry*, 3(1), 32.
83. Teughels W. et al. "Effect of material characteristics and/or surface topography on biofilm development". *Clinical Oral Implants Research* 17.2 (2006): 68-81.
84. Auschill TM, Arweiler NB, Brex M, Reich E, Sculean A, Netuschil L. The effect of dental restorative materials on dental biofilm. *Eur J Oral Sci.* 2002 Feb;110(1):48-53.
85. Scheuerman, T.R.; Camper, A.K.; Hamilton, M.A. Effects of Substratum Topography on Bacterial Adhesion. *J. Colloid Interface Sci.* 1998, 208, 23-33.
86. Netuschil, L., Reich, E. and Brex, M. (1989), Direct measurement of the bactericidal effect of chlorhexidine on human dental plaque. *Journal of Clinical Periodontology*, 16: 484-488.
87. Orstavik D, Kraus FW, Henshaw LC. In vitro attachment of streptococci to the tooth surface. *Infect Immun.* 1974 May;9(5):794-800.
88. Barton, A. J., Sagers, R. D., & Pitt, W. G. (1996). Bacterial adhesion to orthopedic implant polymers. *Journal of Biomedical Materials Research*, 30(3), 403-410.
89. Hannig M, Joiner A. The structure, function and properties of the acquired pellicle. *Monogr Oral Sci.* 2006; 19:29-64.
90. S. Bernardi, S. Bianchi, A. R. Tomei, M. A. Continenza, and G. Macchiarelli, "Microbiological and SEM-EDS evaluation of titanium surfaces exposed to periodontal gel: in vitro study," *Materials (Basel)*, vol. 12, no. 9, 2019.

Eidesstattliche Versicherung

„Ich, Modar Othman versichere an Eides statt durch meine eigenhändige Unterschrift, dass ich die vorgelegte Dissertation mit dem Thema: „Evaluation of the plaque affinity of different PEEK grades in comparison to titanium and zirconium dioxide“ selbstständig und ohne nicht offengelegte Hilfe Dritter verfasst und keine anderen als die angegebenen Quellen und Hilfsmittel genutzt habe.

Alle Stellen, die wörtlich oder dem Sinne nach auf Publikationen oder Vorträgen anderer Autoren/innen beruhen, sind als solche in korrekter Zitierung kenntlich gemacht. Die Abschnitte zu Methodik (insbesondere praktische Arbeiten, Laborbestimmungen, statistische Aufarbeitung) und Resultaten (insbesondere Abbildungen, Graphiken und Tabellen) werden von mir verantwortet.

Ich versichere ferner, dass ich die in Zusammenarbeit mit anderen Personen generierten Daten, Datenauswertungen und Schlussfolgerungen korrekt gekennzeichnet und meinen eigenen Beitrag sowie die Beiträge anderer Personen korrekt kenntlich gemacht habe (siehe Anteilserklärung). Texte oder Textteile, die gemeinsam mit anderen erstellt oder verwendet wurden, habe ich korrekt kenntlich gemacht.

Meine Anteile an etwaigen Publikationen zu dieser Dissertation entsprechen denen, die in der untenstehenden gemeinsamen Erklärung mit dem/der Erstbetreuer/in, angegeben sind. Für sämtliche im Rahmen der Dissertation entstandenen Publikationen wurden die Richtlinien des ICMJE (International Committee of Medical Journal Editors; www.icmje.org) zur Autorenschaft eingehalten. Ich erkläre ferner, dass ich mich zur Einhaltung der Satzung der Charité – Universitätsmedizin Berlin zur Sicherung Guter Wissenschaftlicher Praxis verpflichte.

Weiterhin versichere ich, dass ich diese Dissertation weder in gleicher noch in ähnlicher Form bereits an einer anderen Fakultät eingereicht habe.

Die Bedeutung dieser eidesstattlichen Versicherung und die strafrechtlichen Folgen einer unwahren eidesstattlichen Versicherung (§§156, 161 des Strafgesetzbuches) sind mir bekannt und bewusst.“

Datum

Unterschrift

Für die Unterstützung ohne Ende, die Bereitstellung des Themas sowie die Betreuung gilt mein besonderer Dank mein Doktorvater Herrn Prof. (UH)PD Dr.rer. nat Wolf-Dieter Müller.

Für die Aufmerksamkeit, Nachverfolgung und die Prüfung sowie die Betreuung mein besonderer Dank an Priv.-Doz. Dr. Andreas Schwitalla.

Für die Unterstützung und der Glaube in die Fähigkeiten von Menschen, die Logistik, organisierte und professionelle Verstärkung, den Unternehmergeist, die gute Laune und die anderen aufzunehmen, mein besonderer Dank an Frau Dr.Ing. Franziska Schmidt.

Für das unbegrenzte Geben, die schöne Kameradschaft und die Ideen, die von einem anderen Planeten kommen mein besonderer Dank an Herrn Dr. Matthias Gabriel.

Für die Biologische Informationen, die Materialien besorgen mein besonderer Dank an Herrn Prof. Dr. A.Schäfer.

Für die Hilfe im Rahmen der Ausmessungen mein bester Dank an Frau Dr. Lucia Nascimento.

Für die unbegrenzte Hilfe, die wertvolle Infos und die beste Verstärkung mein besonderer Dank an Herr Sir Avi.

Die Familie ist immer heilig, herzlichen Dank an meine Eltern, mein Vatersaufmerksamkeit und die Bittgebete meiner Mutter, meine Geschwister, Aous und Amjad, mein bester Freund Marcel, der Godfather Dr. Faiz Al-Atiki der mehr als ein Freund ist, und die besondere Hilfe seit dem Anfang um alles zu ermöglichen, Frau Dr. Rim Hmaidouch und an meine Frau, die immer an mich gedacht hat und niemals von mir die Hoffnung abgegeben, für die lange Nächte die sie mit mir warten sollte, für die ganze Unterstützung und motivieren, ich bin stolz auf dich, mein Lieblings Mensch in dieser Welt, Mary...Danke von Herzen.